

Generalized Approximate Message Passing for Unlimited Sampling of Sparse Signals

Osman Musa^{†*}, Peter Jung[†] and Norbert Goertz^{*}

[†]Communications and Information Theory, Technische Universität Berlin

^{*}Institute of Telecommunications, Technische Universität Wien

Email: {osman.musa,norbert.goertz}@nt.tuwien.ac.at, peter.jung@tu-berlin.de

Abstract—In this paper we consider the generalized approximate message passing (GAMP) algorithm for recovering a sparse signal from modulo samples of randomized projections of the unknown signal. The modulo samples are obtained by a self-reset (SR) analog to digital converter (ADC). Additionally, in contrast to previous work on SR ADC, we consider a scenario where the compressed sensing (CS) measurements (i.e., randomized projections) are sent through a communication channel, namely an additive white Gaussian noise (AWGN) channel before being quantized by a SR ADC. To show the effectiveness of the proposed approach, we conduct Monte-Carlo (MC) simulations for both noiseless and noisy case. The results show strong ability of the proposed algorithm to fight the nonlinearity of the SR ADC, as well as the possible additional distortion introduced by the AWGN channel.

Index Terms—Generalized approximate message passing, self-reset analog to digital converter, noisy channel, compressed sensing, Bernoulli-Gaussian mixture

I. INTRODUCTION

Whittaker-Nyquist-Kotelnikov-Shannon theorem is the fundamental result in signal processing, that states that one can perfectly reconstruct a continuous bandlimited signal from a set of samples, taken at a sampling rate which is proportional to bandwidth of the signal. Here we assume that the analog to digital converter (ADC) has infinite precision and infinite dynamic range. Even though, the theory of finite precision quantization (rate distortion theory) is well known for decades, the effects of finite dynamic range (i.e., clipping) became interesting only recently in different research communities, e.g., in image and audio processing, bio-medical applications and analysis of physiological data [1]–[3].

To reduce the negative effects of clipping, Bhandari *et al.* [4] propose digitalizing bandlimited signals with a self-reset (SR) ADC with an appropriate choice of the threshold parameter λ . The SR ADC with the parameter λ is defined by the mapping

$$\mathcal{M}_\lambda(t) = 2\lambda \left(\left\lfloor \frac{t}{2\lambda} + \frac{1}{2} \right\rfloor - \frac{1}{2} \right), \quad (1)$$

where $\lfloor t \rfloor \triangleq t - [t]$ is the remainder of the division t and λ .

In Fig. 1 we illustrate the effects of digitalization with SR ADC, where one can observe that only values of the received signal that are outside the range $[-\lambda, \lambda]$ are affected by the ADC in the sense that the input value is folded to the range $[-\lambda, \lambda]$. If some estimate of the norm of the input signal is known, the authors of [4] prove that perfect recovery of a bandlimited signal from its discrete samples is possible

if the sampling period $T \leq (2\pi e)^{-1}$, where it is assumed that the bandwidth of the signal is normalized to π . Apart from giving the sufficient conditions for perfect recovery, the authors present a stable recovery algorithm.

When sampling certain sparse signals, it was reported in [5]–[8], that during the calibration phase, the received amplitudes are typically larger than during the subsequent sensing phase. Unlike classical approaches of clipping or saturation, the authors in [5] provide sufficient conditions for perfect recovery of K -sparse¹ signal from its low-pass filtered version, together with a constructive recovery algorithm.

Contributions

In this paper we follow the work of [5], but instead of sampling a low-pass filtered version of a sparse signal, we take compressed sensing (CS) measurements and digitalize them with a SR ADC. This problem corresponds to the communication scenario shown in Fig. 2, where we first construct a vector of CS measurements of a sparse signal. That message vector is later transmitted through an additive white Gaussian noise (AWGN) channel and digitalized at the receiver with a SR ADC. To recover the unknown sparse signal we employ the well known generalized approximate message passing (GAMP) [9] algorithm and tailor it to our specific problem. The GAMP algorithm was already successfully applied in [9]–[14] for recovery of sparse signals from CS measurements with nonlinear distortions. To our best knowledge this is the first work that examines the effects of SR ADC on CS phase transition curves.

Notation

Vectors and matrices are represented by boldface characters. Random variables, random vectors, and random matrices are denoted by sans-serif font, e.g., a , \mathbf{a} , and \mathbf{A} , respectively. Function $n(x; \mu, \sigma^2)$ represents a Gaussian pdf with mean μ and variance σ^2 evaluated at x . The Hadamard product (i.e., component-wise multiplication) is denoted by the operator \bullet . If a scalar valued function receives a vector as its argument, this means component-wise application of that function. For example, $\mathcal{M}(\mathbf{z}) = [\mathcal{M}(z_1), \dots, \mathcal{M}(z_n)]^T$, and $(\mathbf{z})^{-1} = [z_1^{-1}, \dots, z_n^{-1}]^T$. The Dirac delta distribution is represented by $\delta(\cdot)$. Unless otherwise specified $\|\cdot\|$ corresponds to the Euclidian (l_2) norm.

¹A K -sparse vector has at most K nonzero components

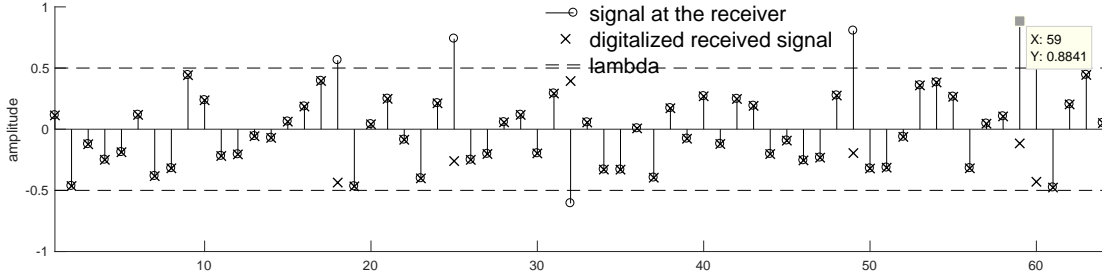


Fig. 1: An example of digitalizing a signal with SR ADC, with $\lambda = 0.5$. All the values inside interval $[-\lambda, \lambda]$ are kept undistorted, while the values outside this range are folded back to the interval $[-\lambda, \lambda]$.

II. SELF RESET ANALOG TO DIGITAL CONVERSION OF CS MEASUREMENTS CORRUPTED WITH AWGN

Next, we formulate the mathematical model for the unknown signal and the measurement process.

A. Signal Model

We assume that the components $\{x_i\}_{i=1}^N$ of the unknown sparse vector \mathbf{x} are i.i.d. realizations of the Bernoulli-Gaussian mixture distribution, i.e.,

$$p_{x_i}(x) = (1 - \epsilon)\delta(x) + \epsilon n(x; 0, \sigma^2), \quad (2)$$

where ϵ represents the probability of nonzero value. Consequently, $1 - \epsilon$ is the sparsity of the signal.

B. Measurement Model

Each measurement y_i is a folded version of the corresponding component i of the received signal \mathbf{y}^* , i.e.,

$$y_i = \mathcal{M}_\lambda(y_i^*), \quad (3)$$

where $\mathcal{M}_\lambda(\cdot)$ represents the nonlinear mapping of the SR ADC converter given in (1). We note that the involved SR ADC has infinite precision in the interval $[-\lambda, \lambda]$. Alternatively, respecting (1) we can write

$$\mathbf{y}^* = \mathbf{y} + \boldsymbol{\epsilon}_g, \quad (4)$$

where the entries of vector $\boldsymbol{\epsilon}_g$ are samples so-called simple function. These samples belong to a set of discrete points $2\lambda\mathbb{Z}$. Furthermore, \mathbf{y}^* is equal to the sum of the vector of CS measurements \mathbf{z} and a noise vector \mathbf{w} , i.e.,

$$\mathbf{y}^* = \mathbf{z} + \mathbf{w} = \mathbf{A}\mathbf{x} + \mathbf{w}, \quad (5)$$

where \mathbf{w} is i.i.d. zero-mean AWGN noise vector with the covariance matrix $\sigma_w^2 \mathbf{I}$, i.e., $\mathbf{w} \sim \mathcal{N}(\mathbf{0}, \sigma_w^2 \mathbf{I})$, and $\mathbf{A} \in \mathbb{R}^{n \times N}$ is the Gaussian measurement matrix, that defines the sampling rate (indeterminacy) $\rho = n/N$. Finally, we can compactly write

$$\mathbf{y} = \mathcal{M}_\lambda(\mathbf{A}\mathbf{x} + \mathbf{w}). \quad (6)$$

Our goal is to estimate \mathbf{x} from \mathbf{y} . To solve this problem we employ the GAMP algorithm that we present in the next section.

III. THE GENERALIZED APPROXIMATE MESSAGE PASSING ALGORITHM OR SELF-RESET ADC

A. The GAMP Algorithm

The equations (7-11) define the steps of the GAMP algorithms [9].

- 1) *Initialization*: At $t = 0$, respecting the prior in (2), the GAMP algorithm is initialized according to

$$\hat{\mathbf{x}}^0 = \mathbb{E}\{\mathbf{x}\} = 0, \quad \mathbf{v}_x^0 = \text{var}\{\mathbf{x}\} = \epsilon \sigma^2, \quad \hat{\mathbf{s}}^0 = \mathbf{y}. \quad (7)$$

- 2) *Iteration*: At every subsequent iteration $t = 1, 2, \dots, t_{\max}$ it performs the measurement updates before the estimation updates, where both updates have a linear step followed by a nonlinear step. Those updates are calculated according to:
 - a) *Measurement update linear step*:

$$\mathbf{v}_p^t = (\mathbf{A} \bullet \mathbf{A}) \mathbf{v}_x^{t-1}, \quad (8a)$$

$$\hat{\mathbf{p}}^t = \mathbf{A} \hat{\mathbf{x}}^{t-1} - \mathbf{v}_p^t \bullet \hat{\mathbf{s}}^{t-1}. \quad (8b)$$

- b) *Measurement update nonlinear step*:

$$\hat{\mathbf{s}}^t = F_1(\mathbf{y}, \hat{\mathbf{p}}^t, \mathbf{v}_p^t), \quad (9a)$$

$$\mathbf{v}_s^t = F_2(\mathbf{y}, \hat{\mathbf{p}}^t, \mathbf{v}_p^t). \quad (9b)$$

- c) *Estimation update linear step*:

$$\mathbf{v}_r^t = ((\mathbf{A} \bullet \mathbf{A})^T \mathbf{v}_s^t)^{-1}, \quad (10a)$$

$$\hat{\mathbf{r}}^t = \hat{\mathbf{x}}^{t-1} + \mathbf{v}_r^t \bullet (\mathbf{A}^T \hat{\mathbf{s}}^t). \quad (10b)$$

- d) *Estimation update nonlinear step*:

$$\hat{\mathbf{x}}^t = G_1(\hat{\mathbf{r}}^t, \mathbf{v}_r^t, p_x), \quad (11a)$$

$$\mathbf{v}_x^t = G_2(\hat{\mathbf{r}}^t, \mathbf{v}_r^t, p_x). \quad (11b)$$

The nonlinear functions in (9) and (11) are applied component-wise and are given by

$$F_1(y, \hat{p}, v_p) = \frac{\mathbb{E}\{z|y\} - \hat{p}}{v_p}, \quad G_1(\hat{r}, v_r, p_x) = \mathbb{E}\{x|\hat{r}\},$$

$$F_2(y, \hat{p}, v_p) = \frac{v_p - \text{var}\{z|y\}}{v_p^2}, \quad G_2(\hat{r}, v_r, p_x) = \text{var}\{x|\hat{r}\}, \quad (12)$$

where

$$f_{z|y} \propto f_{y|z} f_z = f_{y|z} n(\cdot; \hat{p}, v_p),$$

$$f_{x|\hat{r}} \propto f_{\hat{r}|x} f_x = n(\cdot; \hat{r}, v_r) f_x. \quad (13)$$

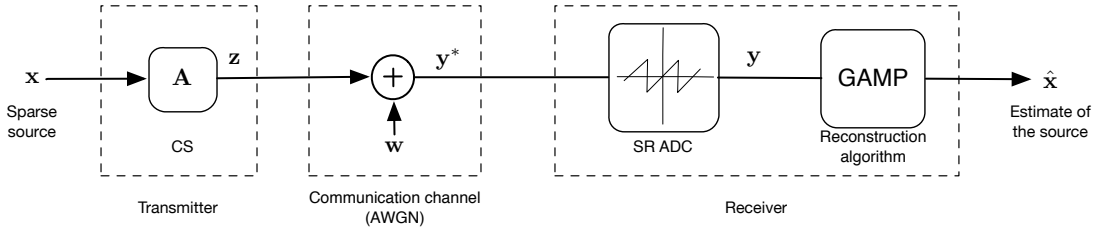


Fig. 2: The signal processing chain. The unknown K -sparse vector $\mathbf{x} \in \mathbb{R}^N$ is multiplied with measurement matrix $\mathbf{A}_{n \times N}$ to obtain a vector of CS measurements $\mathbf{z} \in \mathbb{R}^n$. The components of \mathbf{z} are transmitted through an AWGN channel. At the receiver, the samples of the received signal \mathbf{y}^* are digitalized with a SR ADC to obtain the vector of measurements \mathbf{y} . The GAMP algorithm is applied to produce an estimate $\hat{\mathbf{x}}$ of the unknown sparse signal \mathbf{x} .

	$\mathbb{E}\{z y = y\}$	$\mathbb{E}\{z^2 y = y\}$	$f_y(y)$
SR ADC	$\frac{1}{f_y(y)} \sum_{k=-\infty}^{\infty} (y+2k\lambda) n(y+2k\lambda; \mu_z, \sigma_z^2)$	$\frac{1}{f_y(y)} \sum_{k=-\infty}^{\infty} (y+2k\lambda)^2 n(y+2k\lambda; \mu_z, \sigma_z^2)$	$\sum_{k=-\infty}^{\infty} n(y+2k\lambda; \mu_z, \sigma_z^2)$
AWGN	$\left(\frac{y}{\sigma_w^2} + \frac{\mu_z}{\sigma_z^2}\right) \sigma_{wz}^2$	$\frac{\sigma_w^2 \sigma_z^2}{\sigma_w^2 + \sigma_z^2} + \mathbb{E}\{z y = y\}^2$	$\sum_k n(0; y+2k\lambda - \mu_z, \sigma_z^2 + \sigma_w^2)$

TABLE I: Scalar mean, power, and probability density function for the GAMP nonlinear measurement updates.

3) *Stopping criterion:* We define two criteria for the determining the convergence of the algorithm. We stop iterating if $\|\hat{\mathbf{x}}^t - \hat{\mathbf{x}}^{t-1}\|_2 < \varepsilon \|\hat{\mathbf{x}}^t\|_2$ with a small $\varepsilon > 0$ (e.g., $\varepsilon = 10^{-2}$) or when $t \geq t_{\max}$, where t_{\max} is predefined maximum number of iterations (typically in the order of N or less).

To get more accurate estimate, we use the vector version of the algorithm. Therefore we do not average over the entries of \mathbf{v}_s^t and \mathbf{v}_x^t , given in (9) and (11), respectively.

B. Nonlinear Steps in the Updates

Given the fact that $z \sim \mathcal{N}(\mu_z, \sigma_z^2)$ ² and considering the measurement model given by (6), we can calculate the closed form expressions for the scalar measurement updates in (12). These terms are computed according to Table 1.

The expressions for the nonlinear functions $G_1(\cdot)$ and $G_2(\cdot)$ are identical to those in [13].

IV. NUMERICAL RESULTS

To investigate the performance of the proposed reconstruction algorithm we perform Monte-Carlo (MC) simulations, with the associated parameters described in the following subsection.

A. Simulation Setup

The measurement ratio ρ and the probability of nonzero value ϵ take values in the range $[0.1, 1]$ and $[0.0156, 0.25]$, respectively. For a specific pair $\{\rho, \epsilon\}$, we average results over 4000 independent realizations of sets indices of nonzero components, the values of the nonzero components, the Gaussian sensing matrix \mathbf{A} , and the AWGN \mathbf{w} . The nonzero

components of the source vector \mathbf{x} as well as the entries of the measurement matrix are drawn randomly from a zero-mean Gaussian distribution with power $\sigma^2 = 1$ and $\sigma^2 = 1/n$, respectively. In each simulation we fix $N = 256$, and acquire $n = \rho N$ measurements of the $K = \epsilon N$ sparse vector. Each CS measurement vector is corrupted with AWGN noise with power $\sigma_w^2 = 10^{-\text{SNR}/10}$, where the SNR is defined as

$$\text{SNR/dB} = 10 \log_{10} \{ \|\mathbf{y}^*\|^2 / \|\mathbf{w}\|^2 \}. \quad (14)$$

In the noiseless case, we simply set $\text{SNR} = \infty$. The SR ADC threshold λ is fixed to 1.

The stopping threshold for the algorithms is $\varepsilon = 10^{-3}$, where as the maximal number of iterations of the proposed algorithm is set to $t_{\max} = N/2 = 128$.

To get an insight at recovery potential of the GAMP algorithm, we calculate mean squared error (MSE) for each independent realization of \mathbf{x} , which is defined as

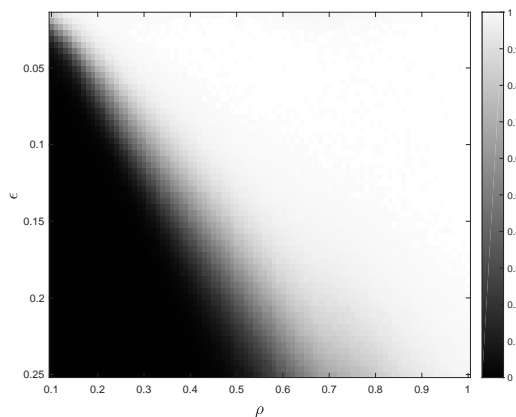
$$\text{MSE/dB} = 10 \log_{10} \|\mathbf{x} - \hat{\mathbf{x}}\|_2^2. \quad (15)$$

In the noiseless case, we calculate the success rate as the average number of successful recoveries. A recovery is considered successful if the resulting MSE is $\leq -30\text{dB}$. We chose this measure of quality of the reconstruction since in the noiseless case, the algorithm either recovers the unknown signal almost perfectly (with very small $\text{MSE} \leq -40\text{dB}$), or fails completely. In the noisy case, MSE is used as a figure of merit.

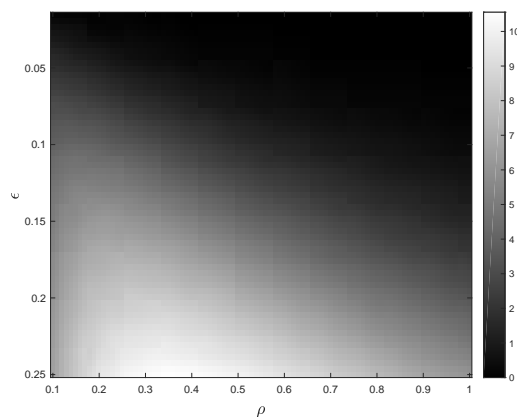
B. Results

Noiseless Case: In Fig. 3, we show the success rate of the GAMP algorithm (Fig. 3a) and the average norm of the simple function $\|\epsilon_g\|_0$ (Fig. 3b), both as a function of the measurement ratio ρ and the nonzero probability ϵ . The norm

²Here we use μ_z and σ_z^2 , instead of \hat{p} and v_p , respectively

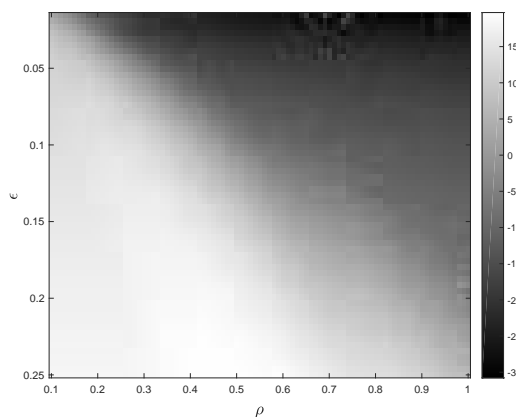


(a) Average success rate of GAMP

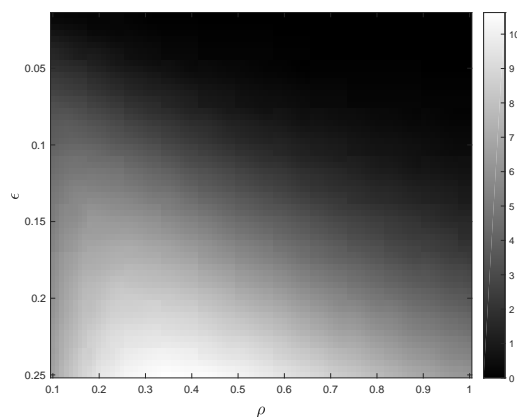


(b) Average norm of the simple function $\|\epsilon_g\|_0$

Fig. 3: Average success rate of GAMP reconstruction algorithm on the left, and average norm of the simple function $\|\epsilon_g\|_0$ on the right as a function of the nonzero probability ϵ and the measurement ratio ρ . The CS measurements are digitalized with a SR ADC with $\lambda = 1$. We consider a reconstruction to be successful if the corresponding reconstruction MSE is ≤ -30 dB.



(a) Average MSE in dB of GAMP



(b) Average norm of the simple function $\|\epsilon_g\|_0$

Fig. 4: Average MSE in dB of GAMP reconstruction algorithm on the left, and average norm of the simple function $\|\epsilon_g\|_0$ on the right as a function of the nonzero probability ϵ and the measurement ratio ρ . The CS measurements are corrupted with AWGN noise before being digitalized with a SR ADC with $\lambda = 1$. The SNR is set to 20dB.

of the simple function provides a measure of how corrupted the measurements are due to SR ADC. In Fig. 3a, we see a clear phase transition between unsuccessful (black) and successful (white) regions. While classical CS algorithms completely fail when $\|\epsilon_g\|_0 \neq 0$, we observe that GAMP is able to cope with folded measurements, and the phase transition is almost linear in ϵ .

Noisy Case: In Fig. 4, we show the MSE of the GAMP algorithm (Fig. 4a) and the average norm of the simple function $\|\epsilon_g\|_0$ (Fig. 4b), both as a function of the measurement ratio ρ and the nonzero probability ϵ . In Fig. 4a we observe that, compared to the noiseless case, the phase transition curve is shifted the right lower corner. This is to be expected, since the measurements are corrupted with AWGN (SNR = 20dB) before digitalization, and more measurements are needed for accurate reconstruction.

Comments: It should be noted that if $\lambda \rightarrow 0$ the measurements become less and less informative, and in the limit

they carry no information. However, taking too large λ , in practical scenarios with finite bit-budget per sample leads to coarse quantization. Hence, one needs to make a good trade-off between large dynamic range and fine quantization resolution. Therefore, it is an interesting research problem to investigate the effects of folding combined with finite bit budget quantization of the measurements on the CS phase transition curves.

V. CONCLUSIONS

In this paper we investigated the potential of applying the GAMP algorithm for recovery of sparse signal from CS measurements digitalized with a SR ADC. Our results show that for certain choice of the signal parameters, the GAMP algorithm is able to successfully recover a sparse signal from folded measurements. Moreover, unlike the previously proposed algorithm for recovery of sparse signals from folded measurements, the GAMP algorithm can cope with the noise introduced by a communication channel.

REFERENCES

- [1] T. Olofsson, "Deconvolution and model-based restoration of clipped ultrasonic signals," *IEEE Transactions on Instrumentation and Measurement*, vol. 54, no. 3, pp. 1235–1240, June 2005.
- [2] F. Esqueda, S. Bilbao, and V. Vlimki, "Aliasing reduction in clipped signals," *IEEE Transactions on Signal Processing*, vol. 64, no. 20, pp. 5255–5267, Oct 2016.
- [3] A. Adler, V. Emiya, M. G. Jafari, M. Elad, R. Gribonval, and M. D. Plumbley, "A constrained matching pursuit approach to audio declipping," in *2011 IEEE International Conference on Acoustics, Speech and Signal Processing (ICASSP)*, May 2011, pp. 329–332.
- [4] A. Bhandari, F. Kraemer, and R. Raskar, "On unlimited sampling," in *2017 International Conference on Sampling Theory and Applications (SampTA)*, July 2017, pp. 31–35.
- [5] A. Bhandari, F. Kraemer, and R. Raskar, "Unlimited sampling of sparse signals." *IEEE SigPort*, 2018. [Online]. Available: <http://sigport.org/3188>
- [6] A. Bhandari, A. M. Wallace, and R. Raskar, "Super-resolved time-of-flight sensing via fri sampling theory," in *2016 IEEE International Conference on Acoustics, Speech and Signal Processing (ICASSP)*, 2016, pp. 4009–4013.
- [7] C. R. Anderson, S. Venkatesh, J. E. Ibrahim, R. M. Buehrer, and J. H. Reed, "Analysis and implementation of a time-interleaved adc array for a software-defined uwb receiver," *IEEE Transactions on Vehicular Technology*, vol. 58, no. 8, pp. 4046–4063, Oct 2009.
- [8] H. M. Jol, *Ground Penetrating Radar Theory and Applications*. Amsterdam: Elsevier, 2009, an optional note.
- [9] S. Rangan, "Generalized approximate message passing for estimation with random linear mixing," in *2011 IEEE International Symposium on Information Theory Proceedings*, July 2011, pp. 2168–2172.
- [10] U. S. Kamilov, A. Bourquard, A. Amini, and M. Unser, "One-bit measurements with adaptive thresholds," *IEEE Signal Processing Letters*, vol. 19, no. 10, pp. 607–610, Oct 2012.
- [11] J. Ziniel, P. Schniter, and P. Sederberg, "Binary linear classification and feature selection via generalized approximate message passing," *IEEE Transactions on Signal Processing*, vol. 63, no. 8, pp. 2020–2032, April 2015.
- [12] U. Kamilov, V. Goyal, and S. Rangan, "Message-passing de-quantization with applications to compressed sensing," *IEEE Trans. on Signal Processing*, vol. 60, no. 12, pp. 6270–6281, Dec. 2012.
- [13] O. Musa, G. Hannak, and N. Goertz, "Efficient recovery from noisy quantized compressed sensing using generalized approximate message passing," in *2017 IEEE 7th International Workshop on Computational Advances in Multi-Sensor Adaptive Processing (CAMSAP)*, Dec 2017, pp. 1–5.
- [14] O. Musa, G. Hannak, and N. Goertz, "Generalized approximate message passing for one-bit compressed sensing with AWGN camsap!!!" in *2016 IEEE Global Conference on Signal and Information Processing (GlobalSIP)*, Dec 2016, pp. 1428–1432.